The Plant Cell, Vol. 26: 1497–1511, April 2014, www.plantcell.org

A Receptor-Like Kinase Mediates Ammonium Homeostasis and Is Important for the Polar Growth of Root Hairs in *Arabidopsis*[W]

Ling Bai,[1] Xiaonan Ma,[1] Guozeng Zhang,[1] Shufei Song, Yun Zhou, Lijie Gao, Yuchen Miao, and Chun-Peng Song[2]

Institute of Plant Stress Biology, State Key Laboratory of Cotton Biology, Department of Biology, Henan University, Kaifeng 475001, China

Ammonium (NH_4^+) is both a necessary nutrient and an important signal in plants, but can be toxic in excess. Ammonium sensing and regulatory mechanisms in plant cells have not been fully elucidated. To decipher the complex network of NH_4^+ signaling, we analyzed $[Ca^{2+}]_{cyt}$-associated protein kinase (CAP) genes, which encode signaling components that undergo marked changes in transcription levels in response to various stressors. We demonstrated that CAP1, a tonoplast-localized receptor-like kinase, regulates root hair tip growth by maintaining cytoplasmic Ca^{2+} gradients. A *CAP1* knockout mutant (*cap1-1*) produced elevated levels of cytoplasmic NH_4^+. Furthermore, root hair growth of *cap1-1* was inhibited on Murashige and Skoog medium, but NH_4^+ depletion reestablished the Ca^{2+} gradient necessary for normal growth. The lower net NH_4^+ influx across the vacuolar membrane and relatively alkaline cytosolic pH of *cap1-1* root hairs implied that mutation of *CAP1* increased NH_4^+ accumulation in the cytoplasm. Furthermore, CAP1 functionally complemented the *npr1* (nitrogen permease reactivator protein) kinase yeast mutant, which is defective in high-affinity NH_4^+ uptake via MEP2 (methylammonium permease 2), distinguishing CAP1 as a cytosolic modulator of NH_4^+ levels that participates in NH_4^+ homeostasis-regulated root hair growth by modulating tip-focused cytoplasmic Ca^{2+} gradients.

INTRODUCTION

To adapt to their limited mobility, plants have evolved complex sensory mechanisms that regulate internal growth, metabolism, and gene expression based on fluctuations in external nutrient concentrations (Forde and Lorenzo, 2001; López-Bucio et al., 2003). For example, root hairs possess intricate regulatory networks that govern cell elongation and employ sophisticated sensory mechanisms that respond to different environment signals. Therefore, root hair cells are an excellent model for investigating the convergence between root hair growth and development and signal sensing (Libault et al., 2010).

The plastic development of root hairs is environmentally regulated, leading to variations in length and density (López-Bucio et al., 2003). Many of the genes encoding transcription factors, protein kinases, and small G proteins involved in root hair initiation and development have been identified (Dolan et al., 1993; Bibikova and Gilroy, 2003; Grierson and Schiefelbein, 2009; Benfey et al., 2010). For example, the transcription factors WEREWOLF (Lee and Schiefelbein, 1999), MYB23 (Kang et al., 2009), and GLABRA3 (Bernhardt et al., 2003) and a Leu-rich repeat receptor-like kinase (RLK) SCRAMBLED (Kwak et al., 2005) function in the differentiation of the root hair cell, where they form a regulatory network that determines the fate of the root epidermal cells (Libault et al., 2010). ROOT HAIRLESS1 is required to initiate root hair development (Schneider et al. 1998). The NADPH oxidase ROOT HAIR DEFECTIVE2 (RHD2/AtrbohC) and the AGC kinase OXIDATIVE SIGNAL-INDUCIBLE1 are essential for establishing the normal morphology of root hairs (Foreman et al., 2003; Rentel et al., 2004).

As in typical polar growth, tip-focused cytoplasmic Ca^{2+} gradients, vesicle/membrane trafficking, cytoskeletal reorganization, and increased oscillations in surface pH and reactive oxygen species (ROS) are involved in root hair elongation (Carol and Dolan, 2002; Monshausen et al., 2007, 2008). The Ca^{2+} gradient localizes newly formed plasma membrane and cell wall to the hair apex, driving cell growth (Carol and Dolan, 2002). Establishing this gradient requires ROS, which are generated by the Respiratory Burst Oxidase Homolog C NADPH oxidase (RHD2/AtrbohC) in *Arabidopsis thaliana* (Foreman et al., 2003). Other ROS generators may assume RHD2's role later in root hair elongation (Monshausen et al., 2007). The *Arabidopsis* loss-of-function mutant for *annexin1* (*ann1*) was found to lack root hairs and epidermal OH-activated Ca^{2+}- and K^+-permeable conductance (Laohavisit et al., 2012).

In plants, many signals are mediated by RLKs. Three of the 17 members of the RLK subfamily CrRLK1L (*Catharanthus roseus* receptor-like-kinase-1-like) mediate cell elongation; knockout or reduction of their expression reduced cell elongation (Guo et al., 2009). Rho-related GTPases of plants (ROPs) also regulate root hair initiation and tip growth by stimulating ROS accumulation (Jones et al., 2002, 2007). Ectopic expression of constitutively active *Arabidopsis ROP11* (*rop11*^{CA}) depolarizes root hair growth, leading to the formation of swollen root hairs (Bloch et al., 2005). High external levels of ammonium (NH_4^+) are essential for the induction of depolarized root hair growth and the activation of downstream

[1] These authors contributed equally to this work.
[2] Address correspondence to songcp@henu.edu.cn.
The author responsible for distribution of materials integral to the findings presented in this article in accordance with the policy described in the Instructions for Authors (www.plantcell.org) is: Chun-Peng Song (songcp@henu.edu.cn).
[W] Online version contains Web-only data.
www.plantcell.org/cgi/doi/10.1105/tpc.114.124586

pathways by rop11^{CA}, suggesting that the coregulation of root hair tip growth by ROP GTPase and by the nitrogen source modulated pH fluctuations (Bloch et al., 2011). A range of transporters in root hairs transport nitrogen, calcium (Ca), potassium (K), and sulfate (Libault et al., 2010).

Nitrogen is an essential macronutrient for plant growth and development, and nitrate (NO_3^-) and NH_4^+ are the dominant forms of inorganic nitrogen in soil. Ammonium is taken up when scarce, but toxic in excess (Loqué and von Wirén, 2004). Therefore, cytoplasmic levels must be tightly controlled through regulated compartmentalization, assimilation, and precise and concerted absorption and excretion using ammonium transporters (AMTs). In the toxic range, NH_4^+ uptake is mediated by a low-affinity transport system. Thus, the rescue of root hair growth in *Atrop11^{CA}* plants by higher NH_4NO_3 levels occurs because the activation of ROP proteins alters NH_4^+ fluxes across the plasma membrane (Bloch et al., 2011). Ammonium uptake was linked to Ca^{2+} release in canola (*Brassica napus*) root cells (Babourina et al., 2007).

The *Arabidopsis* genome encodes six AMTs: AMT1.1 to AMT1.5 and AMT2.1, four of which (AMT1.1, AMT1.2, AMT1.3, and AMT1.5) are involved in NH_4^+ uptake (Yuan et al., 2007). Transcriptional and posttranscriptional regulation of AMTs prevents excess NH_4^+ accumulation and toxicity (Gazzarrini et al., 1999; Loqué et al., 2006, 2009). *AMT1.1* expression is activated by nitrogen deficiency, and phosphorylation of a specific threonine residue exhibits an allosteric effect on AMT and prevents excess NH_4^+ accumulation. This feedback mechanism modulates NH_4^+ uptake in roots over a wide range of nutrient levels (Lanquar et al., 2009), suggesting that roots use either the AMT itself or another extracellular sensor to measure NH_4^+ concentrations in the rhizosphere.

Unlike the NH_4^+ uptake system, the mechanisms by which cytoplasmic NH_4^+ concentrations ($[NH_4^+]_{cyt}$) are regulated to prevent excess accumulation are poorly documented. Indeed, reported $[NH_4^+]_{cyt}$ obtained by physiological experiments are controversial. Millimolar values of $[NH_4^+]_{cyt}$ have been measured using NMR, efflux analysis, ion-specific microelectrodes, and tissue fractionation (Fentem et al., 1983; Lee and Ratcliffe, 1991; Wang et al., 1993; Wells and Miller, 2000). However, because of the potential toxicity of NH_4^+, $[NH_4^+]_{cyt}$ is assumed to be maintained at very low (submillimolar) levels via the high activity and high affinity for NH_4^+ of Gln synthetase (Pearson and Stewart, 1993; Gerendás et al., 1997). Ammonium uptake alkalinizes the cytoplasmic medium, although its assimilation per se is proton neutral (Britto and Kronzucker, 2005). The observations that millimolar NH_4^+ concentrations inside the vacuole largely exceeded those of the cytoplasm in *Chara corallina* cells (Wells and Miller, 2000) and that rape plants showed a large increase in NH_4^+ concentrations in xylem sap when supplied NH_4^+ as a major nitrogen source (Finnemann and Schjoerring, 1999) suggest that NH_4^+ is also exported from the cytoplasm into the apoplasm or the vacuole. In fact, two *Arabidopsis* genes, *TIP2;1* and *TIP2;3*, which encode aquaporins of the tonoplast intrinsic protein (TIP) subfamily, conferred tolerance to the toxic NH_4^+ analog methylammonium in yeast and facilitated NH_3 transport into the vacuole (Loqué et al., 2005). However, much remains to be discovered about how cytoplasmic NH_4^+ levels are sensed and regulated in plant cells.

Using the *Arabidopsis* root hair system, we show that a $[Ca^{2+}]_{cyt}$-associated protein kinase (CAP1) in the CrRLK1L family, functioning as a component of NH_4^+ signaling, can detect internal NH_4^+ status and downregulate the activity of the tonoplast transporter to avoid toxic accumulation of NH_4^+ by sequestering it into the vacuole. CAP1 regulates root hair tip growth by maintaining cytoplasmic Ca^{2+} gradients in the root hair cells. Knockouts of *CAP1* did not produce normal root hairs on Murashige and Skoog (MS) medium unless NH_4^+ was depleted. The depletion of environmental NH_4^+ could reestablish the normal cytoplasmic Ca^{2+} gradient, suggesting that NH_4^+ functions in the polar growth of root hairs. This study identified a novel regulator in the tonoplast for NH_4^+ homeostasis that is distinct from the plasma membrane transceptor for NH_4^+ acquisition (Lanquar et al., 2009).

RESULTS

CAP1 Deficiency Impairs Root Hair Growth

One of the earliest events in a plant's response to hormones, development, or environmental stresses is a rapid, transient elevation of the free cytosolic concentration ($[Ca^{2+}]_{cyt}$) of the intracellular second messenger calcium (Hetherington and Brownlee, 2004; DeFalco et al., 2010). Many protein kinases are involved in regulating $[Ca^{2+}]_{cyt}$ in early signaling. We performed a survey for protein kinase gene expression from the Microarray data using the AtGenExpress Visualization Tool (http://jsp.weigelworld.org/expviz/expviz.jsp) (Kilian et al., 2007). Fifty protein kinase genes that were significantly induced (more than 5-fold) by different stressors (e.g., cold, drought, and salt) were randomly selected. T-DNA insertion mutants of these kinase genes were obtained from the ABRC (Alonso et al., 2003). To identify their role in sensing and regulating responses, we generated transgenic *Arabidopsis* plants that expressed cytosolic aequorin in the T-DNA insertion lines (Knight et al., 1991). Protein kinase mutants containing calcium indicators combined with Ca^{2+} imaging techniques represent a powerful tool to monitor spatial and temporal $[Ca^{2+}]_{cyt}$ to investigate the molecular basis of cell sensing. Mutants with abnormal resting $[Ca^{2+}]_{cyt}$ and/or stimulated increase in $[Ca^{2+}]_{cyt}$ in responses to a specific stressor were selected for further analysis (McAinsh et al., 1992). One of the T-DNA insertion mutants, designated *cap1-1* ($[Ca^{2+}]_{cyt}$-associated protein kinase) (Supplemental Figure 1A), was chosen for detailed characterization because of its low level of resting $[Ca^{2+}]_{cyt}$ as indicated by luminescence levels in seedlings (Supplemental Figure 1C).

CAP1, a member of the CrRLK1L family, has no intron. The homozygous Salk_083442 T-DNA insertion line was first tested by PCR. T-DNA was inserted 1047 bp from the start codon ATG (Supplemental Figure 1A). In an RT-PCR analysis using total RNA extracted from roots, the transcript size (~650 bp) detected on a 1% agarose gel was almost identical for *cap1-1* and the wild type (Supplemental Figure 1B, left panel). However, sequencing of the RT-PCR products showed that 28 bp (from 1422 to 1449) in the mutant cDNA were deleted (Supplemental Figure 1D), resulting in a defective CAP1. To discriminate between the different transcripts produced in the wild type and *cap1-1*, smaller fragments (~250 bp) across this deletion region were amplified and separated on 4% agarose gel. Wild-type

transcripts displayed relatively slower mobility (Supplemental Figure 1B, right panel).

Interestingly, we found that root hairs of *cap1* mutants do not elongate (Figure 1). Root hair growth can be subdivided into three major stages: root hair initiation, transition (slow growth phase), and tip growth (fast growth phase) (Dolan et al., 1994). In each stage, significant differences in root hair length and morphology were found between the wild type and mutant (Figure 1). Compared with the wild type, 7-d-old seedlings of *cap1-1* exhibited 6-fold shorter root hairs (*cap1-1*, 83 ± 8 μm; wild type, 566 ± 34 μm; $P < 0.01$, Dunnett's test; Figure 1B), slightly fewer root hairs (*cap1-1*, 64 ± 1.6; wild type, 80 ± 1.4; $P < 0.01$; Figure 1B), and swollen bases during root hair initiation and abnormal shapes during the fast growth phase (Figure 1C). The mutation of *CAP1* seemed to specifically affect tip elongation and root hair initiation but not cell viability. No other significant differences were observed in adult plants. These results suggested that CAP1 functions in the tip growth of root hairs.

To confirm this conclusion, wild-type *CAP1* was introduced into the mutant under control of the 35S promoter. Transgenic seedlings (*#1* and *#2* in Figure 1A) displayed complementary root hair numbers, lengths, and morphology to the wild type. RT-PCR of these transgenic lines (Supplemental Figure 1B) showed that these seedlings harbored the wild-type coding sequence (Supplemental Figure 1E). The root hair phenotype was also complemented by the expression of wild-type *CAP1* driven by its own promoter (*Com-1* and *Com-2*; Supplemental Figures 2A and 2B). To further ascertain the function of CAP1, we established a set of *CAP1*-suppression transgenic lines using RNA interference (RNAi). The independent transgenic plants (*CAP1-RNAi1*, *2*, or *3* lines) had distinctly fewer root hairs and abnormally swollen bases compared with the wild type (Supplemental Figure 2C), confirming that deficient expression of functional CAP1 was responsible for the mutant phenotype.

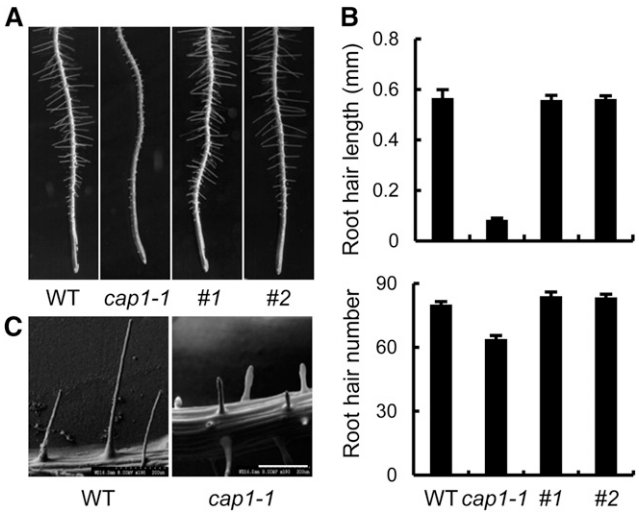

Figure 1. Mutation of *CAP1* Impairs Root Hair Growth in *Arabidopsis*.

(A) Root hair growth of the wild type (WT), mutant (*cap1-1*), and complementation lines (#1 and #2). Seedlings were grown on vertical 1.2% agar MS medium for 7 d.

(B) Comparison of root hair lengths and numbers between the wild type, *cap1-1*, and complementation lines. Root hair lengths were measured in 7-d-old seedlings 5 mm from the primary root tips. Data bars represent means ± SE of root hair lengths from triplicate experiments (wild type and *cap1-1*, $n = 100$; complementation lines, $n = 60$).

(C) Scanning electron micrographs of wild-type and *cap1-1* root hairs. Bar = 200 μm.

Ca^{2+} Gradient and Flux Disappeared in the Root Hair Tips of *cap1-1*

The tip-focused cytoplasmic Ca^{2+} gradient in root hairs regulates root hair growth (Schiefelbein et al., 1992). The Ca^{2+} concentration in *Arabidopsis* root hair tips increased from 200 nM to at least 1 μM (Wymer et al., 1997). We found that $[Ca^{2+}]_{cyt}$ in *cap1-1* seedlings was lower than in the wild type (Supplemental Figure 1C). To understand the regulatory mechanism shaping mutant root hairs, cytoplasmic Ca^{2+} was detected by fluorescence resonance energy transfer based on YC3.6 (Yellow Cameleon 3.6) transformed plants (Monshausen et al., 2008). Consistent with the above results obtained by examining luminescence levels in seedlings, root hair cells and their adjacent epidermal cells in *cap1* mutants showed lower levels of $[Ca^{2+}]_{cyt}$ than did the wild type (Supplemental Figure 3A). Furthermore, we found that growing wild-type root hairs displayed the typical tip-focused Ca^{2+} gradient in all three major growth stages (Figures 2A and 2B), with oscillating Ca^{2+} levels at the tip (Supplemental Figure 3B). In contrast, no such gradients were seen in *cap1-1* mutants (Figures 2A and 2B; Supplemental Figure 3C), suggesting that the absence of a tip-directed Ca^{2+} gradient induced the formation of abnormal root hairs. Therefore, CAP1 plays an important role in establishing a calcium gradient in root hairs.

Calcium ions may be imported across the plasma membrane of root hair tips via channels (Véry and Davies, 2000). Root hairs can import Ca^{2+} from the surrounding solution. We monitored the Ca^{2+} fluxes by the noninvasive micro-test technique (NMT) (Cárdenas et al., 1999) at two positions: the root hair apex (tip) and below the hair's midpoint (base) (Supplemental Figure 4). Inward Ca^{2+} fluxes of around −368 pmol cm^{-2} s^{-1} were recorded at the tip of the wild type, whereas small outward fluxes (60 pmol cm^{-2} s^{-1}) were observed at the base. In contrast, mutant root hairs displayed similar flux values at both the tip and base (51 and 55 pmol cm^{-2} s^{-1}, respectively; Figures 2C and 2D), suggesting that Ca^{2+} levels did not differ in the mutant root hair as a result of calcium channel influx. These results agree with those in YC3.6 transgenic mutant root hairs. The transgenic line (*cap1-1/CAP1*, *#1*) displayed results similar to the wild type (Figures 2C and 2D; −280 and 67 pmol cm^{-2} s^{-1} inward and outward, respectively). This complementation further indicated that CAP1 regulates root hair growth by affecting Ca^{2+} gradient formation.

Deficiency of NH_4^+ Restores Root Hair Growth in *cap1-1*

To pinpoint the causes of root hair growth cessation, we attempted to grow *cap1* mutant plants on MS media with different pH values, containing candidate chemicals such as ethylene and indole-3-acetic acid (both required for root hair elongation) (Pitts et al., 1998), or lacking essential ions such as

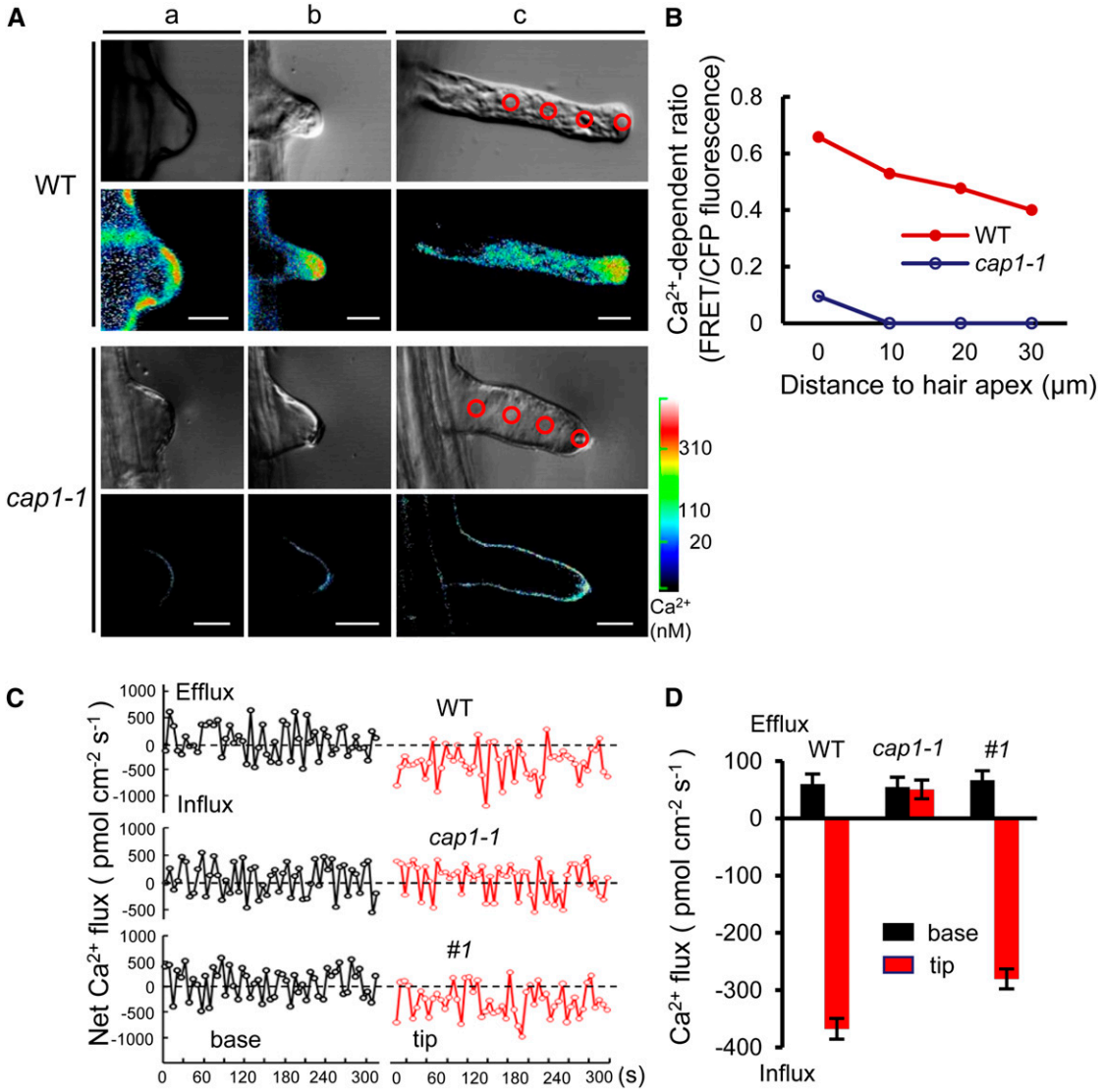

Figure 2. Tip-Focused Ca^{2+} Gradients and Net Fluxes of Ca^{2+} in Root Hair Tips Disappeared in *cap1-1* Mutants.

(A) Tip-focused Ca^{2+} gradients in the cytoplasm of *Arabidopsis* wild-type and *cap1-1* root hairs expressing the Ca^{2+} sensor YC3.6 at different developmental stages (a, initiation phase; b, transition phase; and c, tip growth phase). Bright-field and fluorescence ratio images of Ca^{2+} in root hairs of the wild type and *cap1-1* were obtained as described by Monshausen et al. (2008). Cytosolic Ca^{2+} levels were pseudo-color-coded according to the scale. Representative images of more than 10 measurements from three separate experiments per genotype are presented. Bars = 10 μm.

(B) Quantitative analysis of cytosolic Ca^{2+} levels in a representative growing root hair. Relative Ca^{2+} concentrations were measured in 10-μm^2 regions of interest along lengths of the root hairs in **(A)**, as indicated with circles in the bright-field images. An increase in the fluorescence resonance energy transfer/cyan fluorescent protein ratio based on the Ca^{2+} sensor YC3.6 reflects an increase in cytoplasmic Ca^{2+} level.

(C) Ca^{2+} flux profiles of root hairs in the wild type, *cap1-1*, and *cap1-1/CAP1*. Ion-selective vibration microelectrode recordings of Ca^{2+} fluxes at the surfaces of root hairs of 7-d-old seedlings were made. Graphs show data from positions corresponding to the base (left) and tip (right) of root hairs (Supplemental Figure 4). Trace is a recording of a typical experimental plot illustrating Ca^{2+} influx and efflux in a root hair (inwards, negative; outwards, positive).

(D) Mean fluxes of Ca^{2+} in root hairs. Bars represent means ± SE (n = 5).

iron, K, and phosphate. Surprisingly, *cap1-1* formed wild-type-like root hairs when the MS medium lacked NH_4^+ (wild type, 762 ± 14 μm; *cap1-1*, 725 ± 15 μm; $P > 0.05$, Figures 3A and 3B), whereas other chemicals had no significant effects (Supplemental Figure 5). The *cap1-1* root hair morphogenesis (number, length, and cell pattern) resembled the wild type. To exclude the possibility of nitrogen deprivation, we performed the experiment without NO_3^-. The wild type and *cap1* mutants both had distinctly short root hairs (Figures 3A and 3B). This differential response to nitrogen source has two implications. First, in addition to being an essential nutrient, NH_4^+ functions as a signaling molecule regulating root hair growth. Second, CAP1 serves as an important

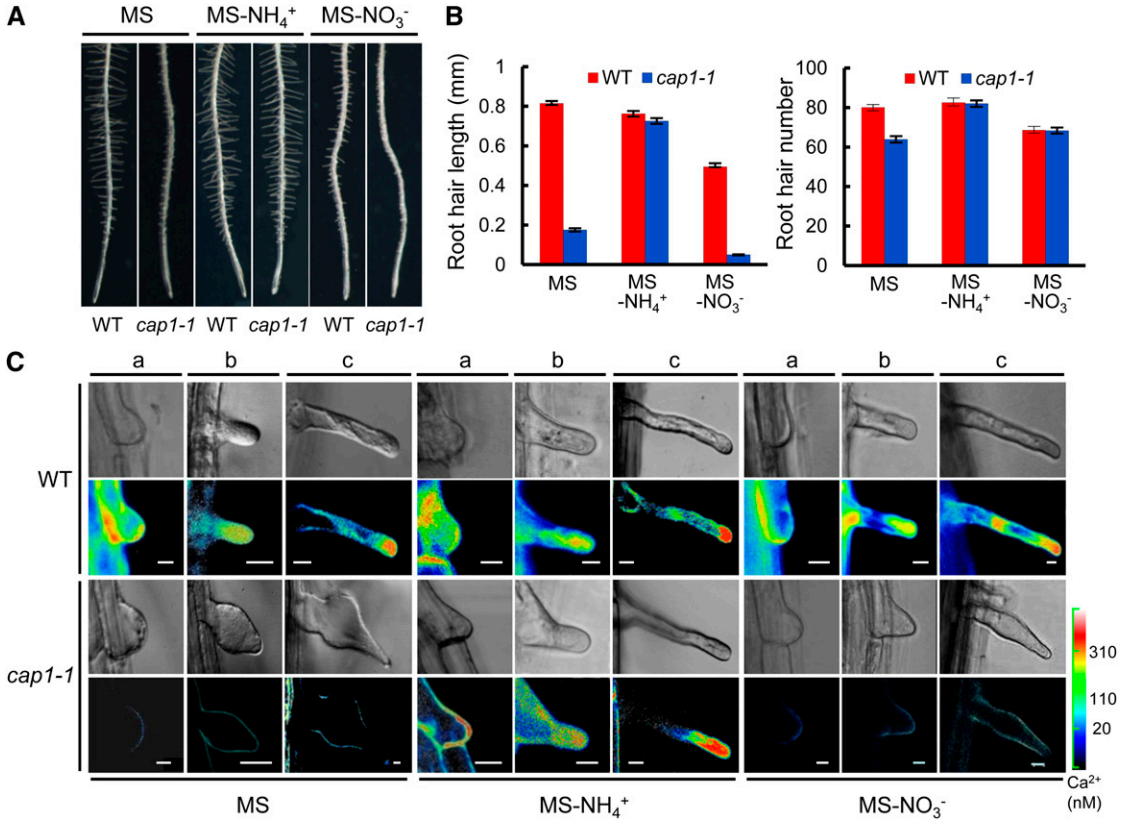

Figure 3. NH_4^+ Deprivation Restored *cap1-1* Root Hair Growth and Tip-Focused Ca^{2+} Gradient.

(A) The absence of NH_4^+, but not NO_3^-, restored root hair growth in *cap1-1*. Seedlings of the wild type and *cap1-1* grown for 7 d on MS, MS lacking NH_4^+ (MS-NH_4^+), and MS lacking NO_3^- (MS-NO_3^-). Root hairs of *cap1-1* were only restored in NH_4^+-free medium.

(B) Comparison of root hair lengths and numbers between the wild type and *cap1-1* on MS, MS-NH_4^+, and MS-NO_3^- media. Data were collected from seedlings grown on MS (n = 100), NH_4^+-free (n = 90), and NO_3^- deprivation (n = 60) media from three separate experiments as described in Figure 1B. Error bars represent means ± SE.

(C) The tip-focused Ca^{2+} gradient was reestablished in YC3.6-transformed *cap1-1* on NH_4^+-free but not on NO_3^- deprivation media. The $[Ca^{2+}]_{cyt}$ of root hairs was measured as described in Figure 2A (a, initiation phase; b, transition phase; and c, tip growth phase). Bars = 10 μm.

modulator for NH_4^+ presence/absence in cells or the external environment.

To elucidate the mechanism of this recovery effect, we monitored root hair Ca^{2+} gradients in seedlings grown in NH_4^+ or NO_3^--deficient media. Interestingly, the root-tip Ca^{2+} gradient and oscillation were reconstituted in the mutant grown in the NH_4^+-deficient medium but not in NO_3^+-deficient medium (Figure 3C; Supplemental Figure 3D), indicating that NH_4^+ affects Ca^{2+} distribution in mutant root hairs, further confirming that CAP1 is involved in an NH_4^+-regulated root hair growth pathway.

CAP1 Is Localized in the Tonoplast and Expressed in Root Hairs

To determine CAP1 localization, mesophyll protoplasts that were transiently transformed with green fluorescent protein (GFP)–tagged CAP1 were observed. Compared with the control transformed with the empty *pHBT-GFP-NOS* vector, cells expressing the CAP1-GFP fusion protein exhibited GFP fluorescence that was distinct from the plasma membrane, strongly suggesting that CAP1-GFP is associated with intracellular membranes. To confirm this, protoplasts were cotransformed with the tonoplast marker γ-TIP1 (Hunter et al., 2007). The merged images of cotransformed protoplasts illustrated the tonoplast localization of the CAP1-GFP fusion protein (Figure 4A). CAP1-GFP fusion protein and GFP empty control were also introduced into onion epidermal cells. Transient expression showed that CAP1 localized in the onion tonoplast, while the epidermal strips transformed with the GFP empty vector fluoresced in a cytosol-rich region (Figure 4B). To confirm the location of CAP1, intact vacuoles were released from protoplasts in hypotonic solutions (Peiter et al., 2005). Fluorescence rapidly dispersed after disruption in protoplasts expressing only GFP (Figure 4C), while it remained associated with the vacuolar membrane in protoplasts expressing CAP1-GFP (Figure 4C), further demonstrating the tonoplast localization of CAP1.

The *CAP1* expression pattern was also tested in transgenic plants expressing β-*glucuronidase* (*GUS*) under control of the *CAP1* promoter. GUS staining showed, and RT-PCR further

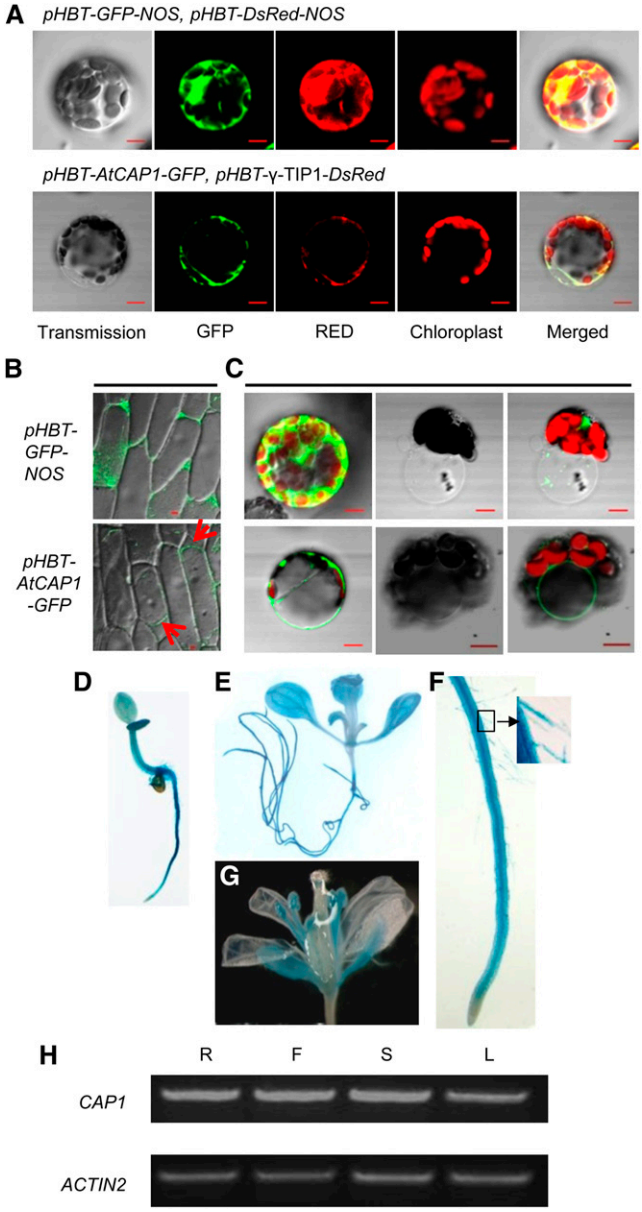

Figure 4. CAP1 Localizes to the Tonoplast and Is Expressed in Root Hairs.

(A) to **(C)** Confocal analysis of the subcellular localization of *CAP1*. Bars = 10 μm.
(A) *CAP1*-fused GFP was transiently coexpressed with the vacuolar membrane marker γ-TIP1 in protoplasts. Images showed colocalization of CAP1 and γ-TIP1 (bottom panels). Empty vector *pHBT-GFP-NOS* expressed in protoplasts was a control (top panels).
(B) Transient expression in onion epidermal cells shows fluorescence of CAP1 in the vacuolar membrane. Arrows point to the vacuole.
(C) Fluorescence images of GFP-transformed protoplast (top panels) and GFP-fused, CAP1-transformed protoplast (bottom panels). The same protoplast before (first image) and immediately after bursting (second two images) is shown.
(D) to **(G)** *CAP1* expression pattern. GUS staining of transgenic plants shows *CAP1* expressed in roots (**[D]** to **[F]**), leaves **(E)**, and flowers **(G)**. Inset image shows root hairs in **(F)**.
(H) RT-PCR indicated that CAP1 was expressed in roots (R), flowers (F), inflorescence stems (S), and young leaves (L).

confirmed, that *CAP1* was universally expressed in most vegetative tissues (Figures 4D to 4H). In roots, strong GUS staining was observed in the maturation and elongation zones, while moderate staining was seen in meristematic zones (Figure 4F). Strong GUS activity was also observed in root hairs and stamens (Figures 4F and 4G).

CAP1 Modulates Ammonium Transport from the Cytoplasm to the Vacuole

Because CAP1 is localized in the vacuolar membrane, it may sense cytoplasmic NH_4^+ levels and modulate the transport system to sequester excess NH_4^+ in the vacuole for detoxification. We used NMT to test net NH_4^+ fluxes of the vacuoles. Vacuoles from root hairs of 7-d-old seedlings were stabilized in a bathing solution for ~10 min. Figure 5A shows the net influx of NH_4^+ uptake (negative net flux) for the wild-type vacuoles (average $I_{in} \approx -97 \pm 16$ pmol·cm^{-2}·s^{-1}, $n = 17$), demonstrating that there was an effective NH_4^+ influx system in the tonoplast. In *cap1-1* vacuoles, net fluxes of NH_4^+ were significantly lower (average -19 ± 10 pmol·cm^{-2}·s^{-1}, $n = 15$; $P < 0.01$, Dunnett's test) than in the wild type (Figure 5A). This implies either decreased influx or increased efflux activity in the vacuole of *cap1-1*.

To determine whether NH_4^+ affected net flux across the tonoplast, vacuoles were obtained from wild-type and *cap1-1* seedlings grown on the NH_4^+-free medium for 7 d. Wild-type vacuoles exhibited an increased NH_4^+ release (positive net flux, average -31 ± 19 pmol·cm^{-2}·s^{-1}, $n = 7$) (Figure 5A). The net flux values of vacuoles in *cap1* plants under NH_4^+-free conditions (23 ± 17 pmol·cm^{-2}·s^{-1}, $n = 9$) were similar to those in the wild type. These flux dynamics showed the ability of wild-type vacuoles to efficiently manipulate cytoplasmic NH_4^+ levels. These data indicated that CAP1 is required to sense NH_4^+ homeostasis and to activate an ion transport system in the tonoplast to sequester excess NH_4^+ in the vacuole.

Because no information was available on the intracellular localization of these changes in NH_4^+ concentration (Speer et al., 1994), two ion-based cytoplasmic measurements were used to estimate the cytoplasmic concentrations of NH_4^+ in the wild type and *cap1-1*. Since extracellular application of NH_4^+ is a standard technique to elevate intracellular pH in animal cells (Boron and De Weer, 1976; Grinstein et al., 1994), root hair cytosolic pH may be alkalinized by equimolar application of NH_4^+ in MS medium. In the first set of experiments, we visualized cytosolic pH (pHc) in root hairs of stable transgenic wild-type and *cap1-1* plants using ratiometric pH-sensitive GFP (Moseyko and Feldman, 2001). Ratio imaging of the pHc indicated a distinct gradient in different root hair developmental stages in the wild type, whose tip zones had relatively alkaline pHc (Figure 5B). As expected, intracellular pH during either the swelling formation or tip growth stages increased significantly after application of 100 mM NH_4^+ for 20 min (Supplemental Figure 7). However, the whole cytoplasm of *cap1-1* root hairs in MS medium had higher pHc (≈8.0) and lacked a pHc gradient. Interestingly, the pHc gradient of mutants was restored in NH_4^+-deficient medium (Figure 5B). These results are consistent with the *cap1* mutant's accumulating more NH_4^+ in the cytoplasm, which disturbed the $[Ca^{2+}]_{cyt}$ and pHc gradients in root hairs.

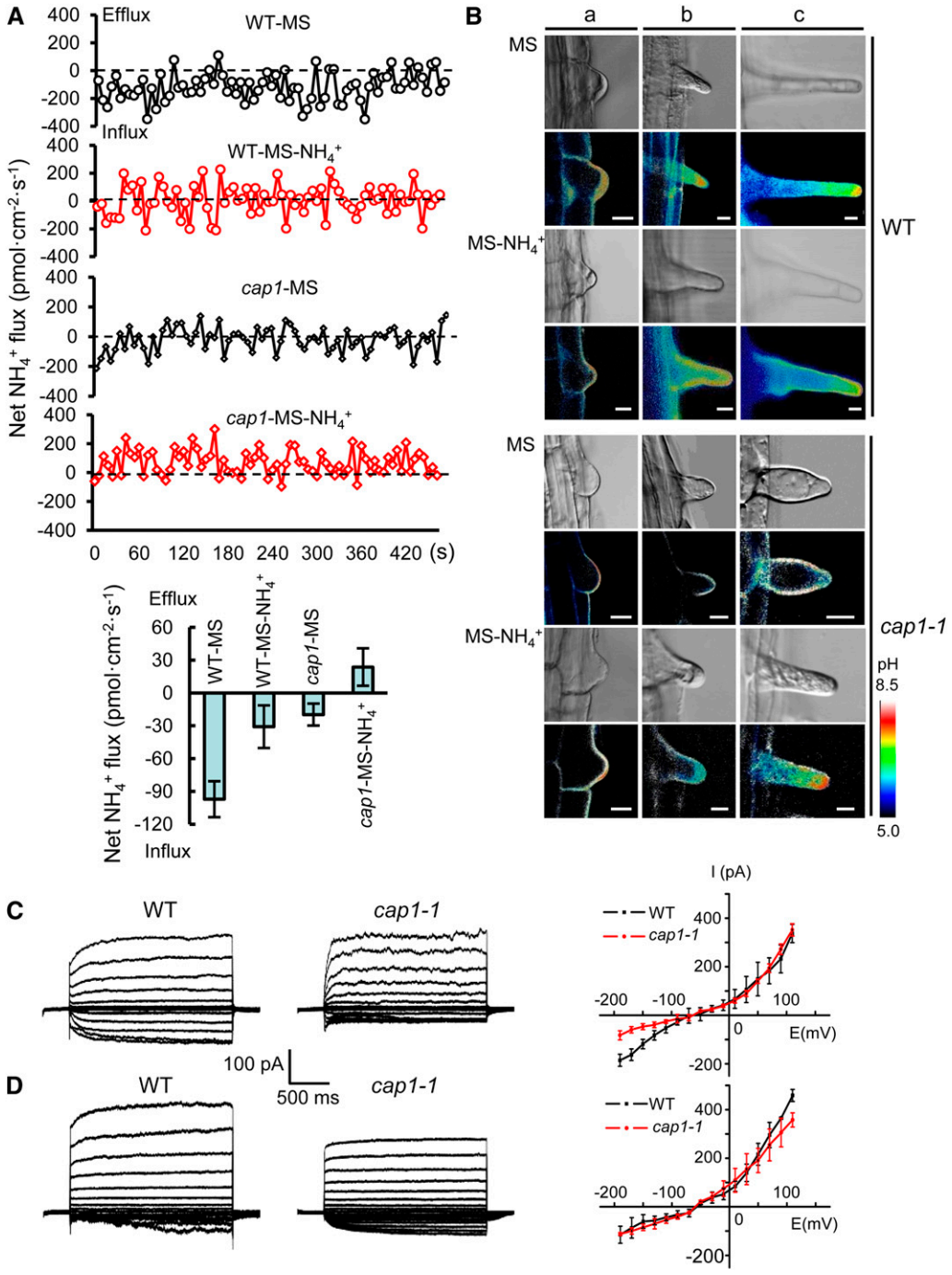

Figure 5. CAP1 Modulates Transportation of Ammonium from the Cytoplasm to the Vacuole.

(A) Changes in NH_4^+ net fluxes of root hair vacuoles (inwards, negative; outwards, positive). Points are data collected every 6 s. Typical net flux traces are shown in the top panel. The NH_4^+ net fluxes are averaged from MS (n = 17 for wild type, n = 15 for *cap1*) and MS-NH_4^+ media (n = 7 for wild type, n = 9 for *cap1*) and plotted in the bottom panel. Error bars represent means ± SE.

(B) Visualizing pHc in root hairs in stable transgenic wild-type and *cap1-1* plants with phGFP using ratiometric pH-sensitive GFP. phGFP accumulates in the peripheral cytoplasm regions near the plasma membrane in *cap1-1* seedling's root hair cells grown on MS medium. pH levels were pseudo-color-coded according to the calibrated 410-nm/470-nm ratio image of the same root hair (Supplemental Figure 6). The different phases of root hair development for the wild type and *cap1-1* are shown: a, the initial phase; b, transition phase; c, tip growth phase. Bars = 10 μm.

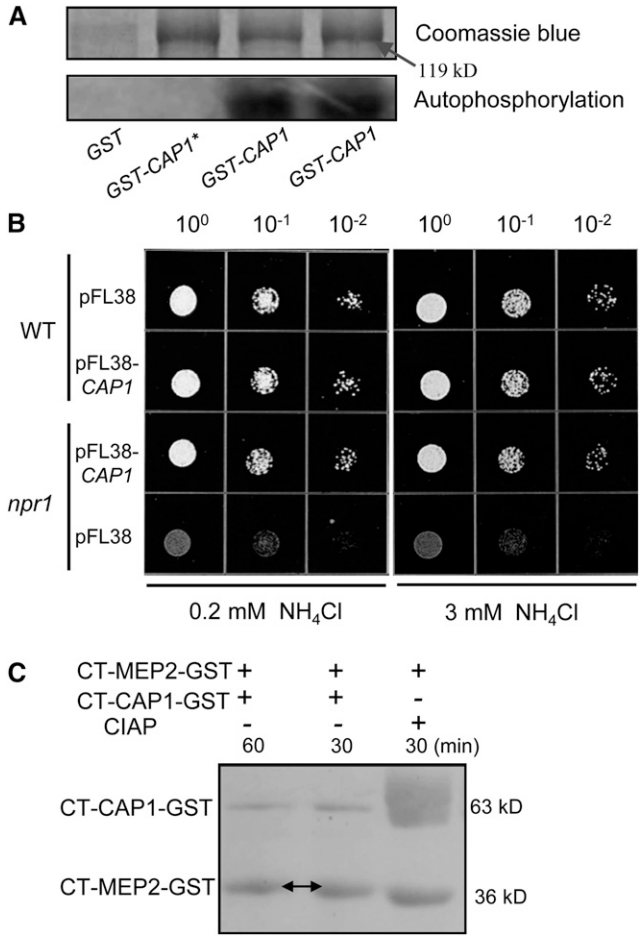

Figure 6. CAP1 Can Be Autophosphorylated and Complements the Activity of NPR1 Kinase in Yeast.

(A) In vitro phosphorylation of CAP1 kinase activity. Recombinant protein fused with GST was used in the kinase assay. Boiled CAP1 protein (GST-CAP1*) was a negative control. Autophosphorylation was detected after protein gel electrophoresis and phosphor imaging.

(B) Growth of yeast strains on solid minimal medium containing different concentrations of NH_4^+ as the sole nitrogen source. Strains 23344c (*ura3*, wild type) and 21994b (*npr1-1*, *ura3*) transformed with plasmid pFL38 and pFL38-*CAP1* were spotted at 10^0-, 10^{-1}-, and 10^{-2}-fold dilutions on YNB medium supplemented with 0.2 and 3 mM NH_4Cl and incubated for 4 d at 29°C.

(C) In vitro kinase assay for MEP2 phosphorylation by CAP1. Recombinant C-terminal fragments of CAP1 (CT-CAP1-GST) and MEP2 (CT-MEP2-GST) were cultured in kinase buffer, and phosphorylated MEP2 exhibited slower mobility (arrows). MEP2 treated with CIAP (alkaline phosphatase) was the control. The phosphorylation reactions were stopped by boiling for 5 min, and the proteins were separated by SDS-PAGE.

To further confirm whether the *cap1-1* cytoplasm accumulated high levels of NH_4^+, we first tried to record the current across the tonoplast using the whole-cell patch clamp technique. However, we could not obtain the NH_4^+ current from the root hair vacuole under our conditions. Ammonium concentration gradients and membrane potentials have been reported to be able to drive the flow of NH_4^+ across plasma membranes (Ludewig et al., 2002, 2003). Therefore, if more NH_4^+ accumulated in the cytoplasm, less should flow across the plasma membrane to the cytosol.

Next, we monitored whole-cell voltage-activated NH_4^+ currents across plasma membranes under standard experimental conditions to indicate the cytoplasmic NH_4^+ levels. Voltage pulses between −190 and 110 mV, in 20-mV increments, were applied to the plasma membrane of a root hair cell protoplast (Figure 5C). An inward current was activated by hyperpolarization of the plasma membrane and an outward current by depolarization. Because Ba^{2+} permeates many Ca^{2+} channels (Gelli and Blumwald, 1997; Klusener and Weiler, 1999), 10 mM Ba^{2+} was supplied in the bathing solution as the charge-carrying ion. In the wild-type root hair protoplast, no significant changes in current were observed (Supplemental Figure 8A). Additional experiments showed that the whole-cell current was not blocked by application of 1 mM La^{3+} (a calcium channel inhibitor) (Supplemental Figure 8B). The data demonstrated that NH_4^+ carried the current, not calcium ions. The *I-V* curves (current-voltage) in Figure 5C (right panel) summarize the data recorded in wild-type and *cap1-1* root hair protoplasts. At a membrane potential of −190 mV, the average inward current of the wild type (−185.7 ± 24.9 pA; $n = 4$) and *cap1-1* (−82.6 ± 18.8 pA; $n = 6$) was significantly different ($P < 0.05$). The lower inward NH_4^+ current of *cap1-1* may imply that mutation of *CAP1* could result in more NH_4^+ accumulating in the cytoplasm.

To confirm this notion, we tried to imitate changes in the cytoplasmic NH_4^+ concentration by replacing 100 mM K-glutamate in the pipette solution with 150 mM NH_4^+-glutamate, as previously described (Murata et al., 2001; Warth et al., 2004). A large reduction of inward current was observed in the wild type. On average, currents of −190 mV decreased to −115.3 ± 35.2 pA, and those of 110 mV increased to 458.3 ± 25.2 pA ($n = 7$). However, currents remained essentially unchanged in *cap1-1* (Figure 5D): Currents at 110 mV were the same ($n = 4$), while those at −190 mV increased by a statistically insignificant amount (from −82.6 ± 18.8 pA to −111.5 ± 51.3 pA; $P > 0.05$).

In the *cap1* mutant, the cytosolic NH_4^+ concentration increased under NH_4^+ nutrition. Thus, the *cap1* mutant is expected to be more sensitive to NH_4^+ toxicity. We therefore analyzed the effects of media with various pH values and high amounts of NH_4^+ on seedling growth. The seeds of the wild type, *cap1-1*, and two complementary lines (*com-1, 2*) were sown on nutrient media with

Figure 5. (continued).

(C) Whole-cell voltage-activated currents in root hair protoplasts of the wild type and *cap1-1* mutants. Typical time-dependent currents recorded in root hair cell protoplasts of the wild type (left) and *cap1-1* (middle) and NH_4^+ current-voltage relationships for the wild type ($n = 4$) and *cap1-1* ($n = 6$) (*I-V* curve, right) are shown. *I-V* curves show means ± SE.

(D) Effects of NH_4^+ on whole-cell currents of wild-type and *cap1-1* root hairs. The data of NH_4^+ application to root hair cells by the addition of 150 mM NH_4^+ to a pipette solution were recorded in the whole-cell patch-clamp configuration (wild type, $n = 7$; *cap1-1*, $n = 4$).

different pH values. The *cap1* mutant was sensitive to either pH 7.0 or pH 5.5 with higher ammonium (NH_4Cl) levels (Supplemental Figure 9), as indicated by severely inhibited seedling growth. Cotyledons did not green on MS medium with a 6-fold concentration of NH_4^+ until the 11th day. Thus, the greater sensitivity to NH_4^+ toxicity of *cap1-1* further supported the conclusion that high levels of NH_4^+ accumulated in its cytoplasm.

CAP1 Can Be Autophosphorylated and Functionally Complement the Activity of Npr1 Kinase in Yeast

To examine the protein kinase activity of CAP1, we constructed glutathione *S*-transferase (GST)–tagged CAP1. CAP1 could autophosphorylate, but boiled CAP1 (the control) could not (Figure 6A). Phosphoproteomics data indicated that CAP1 is a major phosphorylated protein in plants exposed to rapid changes in NO_3^- or NH_4^+ concentrations (Engelsberger and Schulze, 2012). The peptide INIGGDLI(pS)PK of CAP1 corresponds to the conserved malectin domain in the RLK family that controls glucose binding.

In yeast, three Mep-type NH_4^+ transport systems (Mep1, Mep2, and Mep3) are involved in NH_4^+ uptake (Marini et al., 1994; Boeckstaens et al., 2007). MEP2 is a specific NH_4^+ sensor that stimulates pseudohyphal growth during NH_4^+ limitation (Lorenz and Heitman, 1998); its optimal NH_4^+ transport activity requires Npr1 (nitrogen permease reactivator protein) kinase (Boeckstaens et al., 2007), a potential target of rapamycin signaling. Yeast growth in low-NH_4^+ medium is similarly affected in *npr1* mutant cells and in cells lacking the three MEP genes (Feller et al., 2006). The finding that CAP1 functionally perceives NH_4^+ homeostasis in the cytosol raises the possibility that CAP1 resembles MEP2 and Npr1 in yeast and could modulate NH_4^+ signaling to regulate root hair growth. To examine whether CAP1 was activated upon NH_4^+ deprivation, we transferred *CAP1* to yeast strains 23344c (*ura3*) and *npr1* mutant cells 21994b (*npr1-1 ura3*) (Boeckstaens et al., 2007). As shown in Figure 6B, growth of *npr1* was greatly impaired on low-NH_4^+ medium but was rescued by CAP1. To investigate whether MEP2 is a substrate of CAP1, a phosphorylation assay was performed with the recombinant C-terminal tail of MEP2 containing all phosphorylation sites (Van Zeebroeck et al., 2011). As expected, CAP1 could phosphorylate MEP2, while no phosphorylated band was observed in the control protein (Figure 6C). Thus, CAP1, like Npr1 kinase, is required for the optimal uptake activity of NH_4^+ transport systems, indicating that CAP1 is involved in NH_4^+ sensing and transport system activation in plants.

DISCUSSION

Ammonium, both as a necessary nutrient and an important signal in plants, can trigger and regulate a number of critical functions to balance metabolism and uptake at varying nutrient concentrations. The mechanism of NH_4^+ uptake in root hairs has already been established, with AMT family proteins identified as the sole transporters (Lauter et al., 1996; Gazzarrini et al., 1999). However, the precise mechanism by which plants deal with NH_4^+ toxicity remains unknown. Therefore, the exploration of NH_4^+ homeostasis sensing and regulation is an essential and interesting scientific endeavor. Our data identified an important component of the NH_4^+ signaling pathway, CAP1, and provided clues to its precise role in sensing and modulating cytoplasmic NH_4^+ by regulating compartmentation into vacuoles. Indeed, in

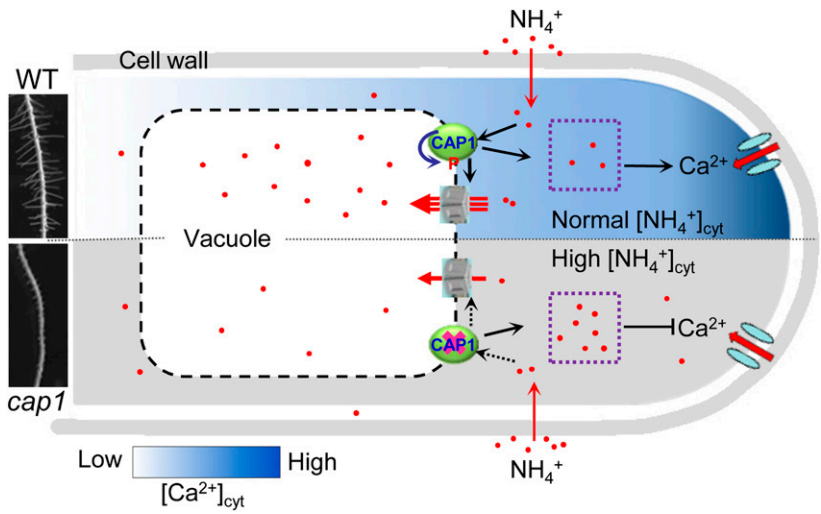

Figure 7. Model Showing the Putative Regulation Pathway of NH_4^+ Homeostasis Mediated by CAP1 in Root Hairs.

In the wild type (in blue), CAP1 in the vacuolar membrane senses cytosolic NH_4^+ levels and phosphorylates an unknown target, such as tonoplast intrinsic protein, resulting in compartmentalization of NH_4^+ in the vacuole and the maintenance of normal NH_4^+ levels in the cytoplasm. Normal NH_4^+ homeostasis is necessary for the establishment of the $[Ca^{2+}]_{cyt}$ gradient in the polar growth of root hairs. When CAP1 was rendered deficient in the mutant (in gray), inward NH_4^+ flux across the vacuole membrane significantly decreased and excess NH_4^+ accumulated in the cytoplasm, causing a loss of calcium gradient (black line with block end) and eventual cessation of root hair growth. The cytosolic Ca^{2+} gradient in the wild type is indicated by the scale below. No gradient was established in *cap1* mutants. Red dots represent ammonium ions. Red lines with arrows indicate ion influx.

cap1 mutants, the presence of NH_4^+ terminated the growth of root hairs (Figure 1), while growth restored in its absence (Figure 3). In addition, the pHc was alkalized in *cap1* mutants (Figure 5B). These data suggested that CAP1 can assess cytoplasmic NH_4^+ levels and phosphorylate an unknown target, such as TIP (Loqué et al., 2005), resulting in compartmentalization. Excess NH_4^+ causes toxicity in plant and animal cells. Vacuole compartmentalization of NH_4^+, which doubles the NH_4^+ concentration in the vacuole compared with the cytoplasm (Loqué and von Wirén, 2004), is important in protecting cells from excess NH_4^+.

The $[Ca^{2+}]_{cyt}$ gradient in root hair cells may be essential for root hair growth (Monshausen et al., 2008; Schiefelbein et al., 1992; Bibikova et al., 1997). Inhibition of this gradient halts growth. In this study, mutant *cap1* had short root hairs and lacked an apparent Ca^{2+} gradient (Figures 1 and 2; Supplemental Figure 3). Consistent with this, calcium fluxes in *cap1*-mutant root hair tips were significantly smaller than in the wild type (Figure 2). The dwarf phenotypes in *herk1 the1* double mutants and *FER* knockdown plants suggested that *HERK1*, *THE1*, and *FER*, members of the CrRLK1L subfamily participate in cell elongation in hypocotyls and petioles (Guo et al., 2009). *ANX1* and *ANX2*, also in the subfamily, specifically regulate the growth of pollen tubes, but not of vegetative tissues (Boisson-Dernier et al., 2009). Another member of the subfamily, *CAP1*, is expressed in root hairs, and serves a similar role in regulating tissue-specific cell elongation, i.e., root hair tip growth.

Our data demonstrated that CAP1 regulates the establishment and maintenance of a Ca^{2+} gradient at the root hair tip, maintaining root hair growth. Analysis of the *cap1* mutant also supported the idea that NH_4^+ is an important factor for maintaining and reestablishing $[Ca^{2+}]_{cyt}$ and pHc gradients in root hairs for polar growth (Figure 3). The tip-focused Ca^{2+} gradient in root hairs is sustained by voltage-gated Ca^{2+} channels (Véry and Davies, 2000) and by ROS (Foreman et al., 2003). Cytoplasmic Ca^{2+} has been shown to decrease in canola root cells when they are taking up NH_4^+ (Babourina et al., 2007). Our results, similar to the observation of Babourina et al. (2007), demonstrated a link between NH_4^+ and Ca^{2+} gradient maintenance through *CAP1* (Figure 3C; Supplemental Figure 3D). Depriving plants of individual nutrients or essential elements proved unsuccessful in restoring tip growth of *cap1* root hairs, with the exception of NH_4^+, indicating that NH_4^+ may serve as a signal for CAP1. Interestingly, on MS medium (which has 20.6 mM NH_4^+), *cap1-1* root hairs could not elongate, but the mutants formed normal root hairs and had normal Ca^{2+} localization when the medium lacked NH_4^+ (Figure 3). The accumulation of NH_4^+ in the cytoplasm may lead to plasma membrane depolarization, resulting in channel activation/deactivation and the consequent formation of a $[Ca^{2+}]_{cyt}$ gradient in root hairs. Therefore, we propose a mechanism in which root hair growth defects in *cap1-1* cells arise through the accumulation of NH_4^+ and impair homeostasis sensing in the cytoplasm. Thus, excess NH_4^+ in the cytoplasm of *cap1-1* mutants will disturb homeostasis by disrupting the establishment of the normal $[Ca^{2+}]_{cyt}$ gradient, halting root hair growth. However, this distinct response to extracellular NH_4^+ by the *cap1* mutant indicates that understanding the signaling pathway of NH_4^+-related CAP1-regulated tip growth may shed light on the mechanism of tip growth.

How CAP1 senses NH_4^+ homeostasis for detoxification is unclear at present. However, our results showed that CAP1 could functionally complement a yeast mutant defective in high-affinity NH_4^+ uptake by *npr1* kinase and showed kinase activity that regulated NH_4^+ transport between the cytoplasm and vacuole (Figures 5 and 6). The amplitude of extracellular and intracellular pH oscillations increases after the addition of NH_4NO_3 to the growth medium, whereas an overall decrease in cytoplasmic pH at the cell apex is induced (Bloch et al., 2011). In animal cells, in contrast, extracellular application of NH_4^+ alkalinizes the cytoplasmic medium (Boron and De Weer, 1976; Grinstein et al., 1994). These findings are consistent with our observation that suddenly imposing a high level of NH_4^+ in MS medium on root hairs elevated intracellular pH (Supplemental Figure 7). In *cap1-1*, a lack of NH_4^+ in the medium reconstituted the pH gradient and restored tip growth of root hairs. Thus, when *CAP1* is defective, the greater accumulation of NH_4^+ and the effects of pH changes arrested root hair growth, which manifested as swollen root hairs. In agreement with a possible effect of CAP1 on regulating NH_4^+ homeostasis in root hairs, we observed that *cap1* mutants were more sensitive than the wild type to higher NH_4^+ concentrations in MS medium (Supplemental Figure 9). One possible mechanism for this modulation is that NH_4^+ accumulation induces the activation of CAP1 for phosphorylation of unknown targets that compartmentalize NH_4^+ into the vacuole.

Based on previous reports and the data presented here, we propose a working model for NH_4^+ detoxification in which CAP1 senses the cytoplasmic NH_4^+ concentration and regulates its uptake and relocation (Figure 7). In the wild type, CAP1 in the vacuolar membrane could sense the NH_4^+ concentration in the cytoplasm and trigger the transporter and/or relocation system in the tonoplast, resulting in the accumulation of NH_4^+ in the vacuole and the maintenance of NH_4^+ homeostasis. When CAP1 was rendered deficient in the mutant, excess NH_4^+ collected in the cytoplasm, causing a loss of calcium gradient and eventual cessation of root hair growth because of toxicity. Our data elucidated an important feature, CAP1, of the NH_4^+ signaling pathway and provided clues to its precise role in sensing and transmitting signals in NH_4^+ homeostasis. In summary, CAP1 is an important NH_4^+ modulator that participates in the pathway of environmental NH_4^+-regulated root hair growth by regulating tip-focused cytoplasmic Ca^{2+} gradients.

METHODS

Plant Materials and Growth Conditions

All *Arabidopsis thaliana* plants used were in the Columbia background. Surface-sterilized seeds were sowed on MS medium and kept for 3 d at 4°C in the dark to break dormancy. To analyze root hair growth, different hormones or ions were added or removed from the medium. The plates were then transferred to a culture room at 22°C with a 16-h-light/8-h-dark photoperiod and grown vertically. The *CAP1* T-DNA insertion line Salk_083442 was obtained from the ABRC.

Constructions and Plant Lines

A gene-specific fragment of *CAP1* cDNA was amplified by PCR. For the *CAP1* overexpression construct, the primers 5′-TTACCCGGGATGGGAGGA-GATTTTCGT-3′ and 5′-TCCGAGCTCTCACGGTATTGAATGCGA-3′ were used. The amplified product was cloned into the pCAMBIAsuper-1300 vector

cut with *Sma*II and *Sac*I. For the GFP reporter vector, the full-length *CAP1* coding sequence was amplified with primers 5′-AAAGGTACCATGGGAGGA-GATTTTCGTCAT-3′ and 5′-TTTCCCGGGAACGGTATTGAATGCGACG-3′ and then cloned into pHBT-GFP vector cut with *Kpn*I and *Sma*II. To generate the *CAP1-GUS* construct, a 619-bp *CAP1* promoter fragment was amplified using primers 5′-GCCGAATTCTCGCTTTGAGGTCATTTT-3′ and 5′-GAACTGCA-GAATATCCGGCGAGGTTTTGAAG-3′, and the PCR product was digested with *Eco*RI and *Pst*I and cloned into pCAMBIA1381 vector. The constructs were introduced into *Agrobacterium tumefaciens* strain GV3101 and transformed by floral infiltration into the wild type (for GUS staining assays) and *cap1-1* mutant (for gene complementation) plants.

To generate the gene silencing vector, 151-bp fragments corresponding to the 5′ coding sequence of *CAP1* were amplified by PCR with the primers CAP1-*Xho*I-S-F (5′-GAACTCGAGCGCTTAACGACCTTATCTT-3′) and CAP1-*Nco*I-S-R (5′-GAACCATGGGTGATCGTAGACGCATTAA-3′) and the primers CAP1-*Sma*I-S-F (5′-TTACCCGGGCGCTTAACGACCTTATCTT-3′) and CAP1-*BamH*I-S-R (5′-TAAGGATCCGGTGATCGTAGACGCATTA-3′). PCR products were digested with *Xho*I-*Nco*I and *Sma*I-*Bam*HI to produce hairpin RNA for *CAP1*. The two fragments were sequentially ligated to the vector pFGC5941-35S-RNAi. The resulting construct was transformed into *Arabidopsis* Columbia-0 (Col-0) mediated by *Agrobacterium GV3101* via the standard floral dip method.

For phosphorylation assays of CAP1 and MEP2, GST-fused plasmid constructions were made. The C termini of CAP1 (1549 to 2529 bp) and MEP2 (1251 to 1500 bp) were amplified with the following primer pairs: forward CT-CAP1-GST (5′-ATAGGTACCGAACTACAGACCGCGACACAA-3′) and reverse CT-CAP1-GST (5′-TTTGAATTCTCACGGTATTGAATGCGACGG-3′), and forward CT-MEP2-GST (5′-ACGGTCGACTTCCATTTTTAAAACTA-AGA-3′) and reverse CT-MEP2-GST (5′-GCGAAGCTTCTTATACTATATG-GTCAGTGT-3′), respectively. The PCR fragments were cloned as *Eco*RI-*Kpn*I (for CT-CAP1-GST) and *Sal*I-*Hin*dIII (for CT-MEP2-GST) restriction fragments in the pGEX-2T *Escherichia coli* expression vector for expressing GST-tagged C-terminal proteins in *E. coli* strain BL21.

Measurement of Root Hair Length

Root hairs were observed in 7-d-old seedlings grown on MS agar plates. Root hair lengths were determined by measuring the five longest root hairs within 5 mm of the root tip of each line. Root hairs were photographed using a FV1000 confocal microscope (Olympus). Root hair lengths were measured using ImageJ (http://rsbweb.nih.gov/ij/).

Calcium Imaging

The 35S promoter-driven YC3.6 vector (in pEarleyGate100 vector) was kindly provided by Simon Gilroy. Ratio images were performed essentially as described previously (Monshausen et al., 2008) using root hairs of wild-type and *cap1-1* transgenic seedlings and the FV1000 confocal microscope. The process of root hair elongation takes ~300 min (Dolan et al., 1994), and focusing on the same root cells through all the growth stages is difficult. Therefore, different root hair cells at different stages were scanned along the root tip.

Subcellular Localization and Histochemical Detection of GUS Activity

For GFP analysis, the final construct pHBT-GFP-AtCAP1 and empty vector pHBT-GFP were transiently expressed in mesophyll protoplasts (Yoo et al., 2007) and in onion epidermal cells using a particle gun–mediated system (Li et al., 2010). For transformation with protoplasts, GFP fluorescence was scanned after vacuoles were released from protoplasts (Peiter et al., 2005). Vacuolar membrane–localized pHBT-γTIP1-DsRED was cotransformed with pHBT-GFP-AtCAP1, and the empty vector pHBT-DsRED was cotransformed with pHBT-GFP for further analysis of CAP1 location. Transgenic cells were examined under the FV1000 confocal microscope. For the GUS assays, excised tissues from 15 independent transgenic lines containing the *CAP1 promoter–GUS* construct were tested according to Song et al. (2005).

Net Ca^{2+} and NH_4^+ Flux Measurements with NMT

Net fluxes were obtained with a BIO-IM Series NMT system (YoungerUSA) at the Xuyue Beijing NMT Research Service Center, China.

Seven-day-old *Arabidopsis* roots cultured in MS media were placed in Petri dishes containing 10 mL of liquid medium (0.1 mM $CaCl_2$, 0.1 mM KCl, 0.1 mM $MgCl_2$, 0.5 mM NaCl, 0.2 mM Na_2SO_4, 0.3 mM MES, and 1% sucrose, pH 6.0), and treated for 20 to 30 min before the Ca^{2+} flux experiments. The same medium was used for net flux measurements throughout our experiments. After primary scans along the root hairs, the root hair tips and middle regions were selected for the measurement of net Ca^{2+} fluxes.

Microelectrodes selective for Ca^{2+} were freshly fabricated prior to the NMT tests. Silanized glass microelectrodes (inner diameter 4 ± 1 μm; YG-IS-ME02; YoungerUSA) were first backfilled with Ca^{2+} solution (100 mM $CaCl_2$) to a length of ~1 cm and then front-filled with 25-μm columns of selective Liquid Ion eXchange (LIX; YG-LIX-Ca01; YoungerUSA). Before and after each flux measurement, the microelectrodes were calibrated with the culture medium with 1, 0.1, and 0.01 mM Ca^{2+}. Only electrodes with a Nernstian slope >26 mV/decade for Ca^{2+} were used in our study.

Seven-day-old seedlings were used for net NH_4^+ flux measurements. Root epidermal cell protoplasts were first isolated from the root hair zones by digesting the zones for 2 to 3 h in 1.5% cellulose RS (Yakult) and 0.075% pectolyase Y-23 (Yakult), and then vacuoles were released by washing these protoplasts with a solution containing 10 mM EDTA and 10 mM EGTA, pH 7.8, with an osmolarity of 120 mOsM adjusted with mannitol. Vacuoles adhered to poly-Lys pretreated cover slides that were presettled in a Petri dish. Vacuoles were gently rinsed with bathing solution (0.1 mM NH_4Cl, 0.1 mM KCl, 0.5 mM NaCl, 0.1 mM $CaCl_2$, 120 mM mannitol, and 0.05 mM MES, pH 7.8) and stabilized in this solution for ~10 min before measurement. Net flux measurements were performed in this solution. Microelectrodes selective for NH_4^+ were freshly made prior to the NMT tests. Silanized glass microelectrodes (diameter 1.5 ± 0.5 μm; XY-DJ-02; YoungerUSA) were first backfilled with NH_4^+ solution (100 mM NH_4Cl) to a length of ~1 cm and then front-filled with 15- to 50-μm columns of selective liquid ion-exchange cocktails (LIX; XY-SJ-NH_4; YoungerUSA). Before measurements, microelectrodes selective for NH_4^+ were first calibrated with bathing solution with 0.05 and 0.5 mM NH_4^+. Only electrodes with a Nernstian slope >53 mV/decade for NH_4^+ were used in our study.

The net ion fluxes were calculated based on Fick's law of diffusion: $J = -D_0 (dc/dx)$, where J is the ion flux (picomoles/cm^2/s), D_0 is the ionic diffusion coefficient of a specific ion in a given medium, dc is the ion concentration difference based on microvolt differences, and dx is the distance the microelectrode moved from one point to another perpendicular to the root hair or vacuole surfaces. The microelectrodes were positioned 1 ± 0.5 μm away from the samples by the computer-controlled NMT system. Net fluxes were calculated using JCal 1.0 (a free MS Excel spreadsheet, http://youngerusa.com/jcal or http://ifluxes.com/jcal).

Yeast Expression

Yeast strains 23344c (*ura3*, wild type) and 21994b (*npr1-1 ura3*) transformed with plasmids pFL38 and pFL38-CAP1 were grown in liquid YPD (yeast extract peptone dextrose) medium at 29°C for ~1 d, diluted 10^{-1}- to 10^{-2}-fold, and dropped on solid Yeast Nitrogen Base W/O amino acids medium (Difco) supplemented with 0.2 and 3 mM NH_4Cl. Yeast cells were incubated for 4 d at 29°C.

Kinase Activity Assay

The recombinant GST-tagged fusion protein was affinity-purified from bacterial BL21 lysate using glutathione sepharose 4B (GE Healthcare). The kinase activities of the fusion proteins were then measured according to the method of Peck (2006).

According to Van Zeebroeck et al. (2011), the GST-tagged C-terminal tail of MEP2 was purified from *E. coli* strain BL21. For the phosphorylation assay, C-terminal proteins of CAP1 and MEP2 were cultured in the kinase buffer (500 mM HEPES, pH 7.4, 100 mM $MgCl_2$, and 20 mM $MnCl_2$) with 10 mM ATP for 30 and 60 min. MEP2 treated with CIAP (alkaline phosphatase; TaKaRa) for 30 min was used as the control. The reactions were stopped by boiling for 5 min, and the proteins were separated by SDS-PAGE.

Whole-Cell Patch Clamping and Data Acquisition

Arabidopsis root hair cell protoplasts were isolated as previously described (Ivashikina et al., 2001). Highly vacuolated root hair cell protoplasts were patch clamped (Véry and Davies, 2000). The bathing solution included 10 mM NH_4-glutamate, 2 mM $CaCl_2$, 4 mM $MgCl_2$, and 5 mM MES, pH 5.6, with osmolality adjusted to 300 mOsM with sorbitol. The standard pipette solution contained 100 mM K-glutamate, 2 mM $MgCl_2$, 2 mM EGTA, 10 mM HEPES, and 2 mM Mg-ATP, pH 7.2, with adjusted osmolality of 420 mOsM. Recording pipettes were made from borosilicate glass capillaries (Kimax-51; Kimble Glass) using a vertical two-stage puller (model PC-10; Narishige) and fire-polished with a microforge (model MF-90; Narishige) before use. Whole-cell NH_4^+-current recordings were performed essentially as described previously (Bei and Luan, 1998; Ivashikina et al., 2001). Data were acquired 15 min after the formation of the whole-cell configuration. Whole-cell currents were measured in response to 3-s voltage pulses from −190 to 110 mV in 20-mV steps using an EPC-9 patch-clamp amplifier (HEKA Elektronik). Whole-cell data were analyzed with the software PLUSE and PLUSEFIT (version 8.3) as described by Zhang et al. (2001).

pHc Imaging

Stable Pt–GFP transgenic wild-type line N9561 (background: Col-0) was obtained from the Nottingham Arabidopsis Stock Centre (http://Arabidopsis.info/StockInfo?NASC_id=9561), and *cap1-1* plants containing pH-sensitive GFP were obtained by crossing with Pt-GFP lines. Root hairs of 4- to 5-d-old seedlings were used to monitor intracellular pH. GFP fluorescence was monitored using a FV1000 confocal microscope (exciters, 410 nm and 470 nm; emitter, 525 nm); the F410-to-F470 ratio was used as a measure of pH. pH levels were pseudo-color-coded according to the calibrated 410-nm/470-nm ratio image of the same root hair. The pH titrations were performed in situ as described by Moseyko and Feldman (2001).

Generation of pMAQ2 Transgenic Plants and Measurements of Ca^{2+} Luminescence

The pMAQ2 plasmid was transformed into *Arabidopsis* Col-0 and the homozygous T-DNA insertion lines mediated by *Agrobacterium GV3101* via the standard floral dip method. Stable transgenic *Arabidopsis* plants expressing cytosolic apoaequorin were used. For $[Ca^{2+}]_{cyt}$ measurements, aequorin was reconstituted in vivo essentially as described previously (Knight et al., 1991) by incubating seedlings in water containing 2.5 μM native coelenterazine (Promega) overnight in the dark at room temperature. One seedling was placed in a transparent plastic cuvette without liquid. The cuvette was placed inside a TD20/20n digital luminometer (Turner Biosystems). Luminescence was recorded every 0.2 s. At the end of each experiment, the remaining aequorin was discharged by adding an equal volume of 2 M $CaCl_2$ and 20% ethanol. Luminescence values were converted to calcium concentrations as described previously (Knight et al., 1996).

CAP1 Expression Analyzed by RT-PCR

RNA was isolated from 100 mg roots using TRIzol reagent (Invitrogen). First-strand cDNA was synthesized using M-MLV reverse transcriptase (Promega). Primers used for CAP1 were: 5′-TTGATGGGAAATACAAAGGAC-3′ and 5′-GGACAAGGTAGGAATAGGGTTA-3′. Another pair of primers for obtaining smaller fragments across the deletion region is: 5′-CGCTAACCGCTTTCTTAGGGGTTGT-3′ and 5′-TCGGTAAAGGGAAAGTACCGACCTA-3′. The cDNA yield was determined by measuring the amount of product that was amplified from an internal standard, the housekeeping gene *Actin2*. Primers used for *Actin2* were: 5′-TTCCTCATGCCATCCTCCGTCTT-3′ and 5′-CAGCGATACCTGAGAACATAGTGG-3′. All PCR reactions were performed in triplicate.

Statistical Analysis

To determine significant differences among different lines or different treatments, all the data were analyzed by Dunnett's test using SPSS16.0 software.

Accession Numbers

Sequence data from this article can be found in the National Center for Biotechnology Information database under the following accession numbers: *Saccharomyces cerevisiae* MEP2 (NM_001182980) and NPR1 (Z71459); *Arabidopsis* gene *CAP1* (At5g61350).

Supplemental Data

The following materials are available in the online version of this article.

Supplemental Figure 1. The *CAP1* T-DNA Insertion Mutant Has a Lower Cytoplasmic Calcium Concentration and BLAST Results of *cap1-1* and Overexpression Transcripts.

Supplemental Figure 2. Root Hair Phenotype Was Complemented by *CAP1* Driven by the Wild-Type Promoter in Mutants and Suppression of *CAP1* Expression in *Arabidopsis* RNAi Knockdown Lines.

Supplemental Figure 3. FRET-Based YC3.6 Shows Levels of $[Ca^{2+}]_{cyt}$ and Oscillation of Tip-Focused Ca^{2+} Gradients Only in Wild-Type Root Hairs.

Supplemental Figure 4. Ion-Selective Vibration Microelectrode Recording of Ca^{2+} Fluxes at Root Hair Surfaces in 7-d-Old Seedlings.

Supplemental Figure 5. Effects of Auxin (IAA), Ethylene (ETH), Various Nutrients, and pH on the Growth of Root Hairs in Wild-Type and *cap1-1* Plants.

Supplemental Figure 6. Standard Curve of the Calibrated 410 nm/470 nm Ratio in Different pH Solutions.

Supplemental Figure 7. High Levels of NH_4^+ Enhances Root Hair pHc.

Supplemental Figure 8. Characterization of Ammonium Current Recording on the Whole-Cell Model Using Ba^{2+} and La^{3+}.

Supplemental Figure 9. *cap1-1* Was More Sensitive to High Levels of Ammonium Than Wild-Type and the Complementary Lines.

ACKNOWLEDGMENTS

We thank Marc R. Knight of Durham University (UK) for the kind gift of pMAQ2 and for his excellent technical assistance and Simon Gilroy of the University of Wisconsin, Madison, for the generous gift of the YC3.6 vector. We also thank Bruno André of Université Libre de Bruxelles for kindly providing Npr1 yeast strains. This work was supported by the National Key Basic Special Funds (2012CB1143001) and the National Natural Science Foundation of China (90817106 and U1204302).

AUTHOR CONTRIBUTIONS

C.-P.S. designed the research. L.B., X.M., G.Z., L.G., Y.Z., and Y.M. performed the research and analyzed data. C.-P.S., L.B., and S.S. wrote the article.

Received February 21, 2014; revised March 30, 2014; accepted April 9, 2014; published April 25, 2014.

REFERENCES

Alonso, J.M., et al. (2003). Genome-wide insertional mutagenesis of *Arabidopsis thaliana.* Science **301:** 653–657.

Babourina, O., Voltchanskii, K., McGann, B., Newman, I., and Rengel, Z. (2007). Nitrate supply affects ammonium transport in canola roots. J. Exp. Bot. **58:** 651–658.

Bei, Q., and Luan, S. (1998). Functional expression and characterization of a plant K^+ channel gene in a plant cell model. Plant J. **13:** 857–865.

Benfey, P.N., Bennett, M., and Schiefelbein, J. (2010). Getting to the root of plant biology: impact of the *Arabidopsis* genome sequence on root research. Plant J. **61:** 992–1000.

Bernhardt, C., Lee, M.M., Gonzalez, A., Zhang, F., Lloyd, A., and Schiefelbein, J. (2003). The bHLH genes *GLABRA3* (*GL3*) and *ENHANCER OF GLABRA3* (*EGL3*) specify epidermal cell fate in the *Arabidopsis* root. Development **130:** 6431–6439.

Bibikova, T.N., and Gilroy, S. (2003). Root hair development. J. Plant Growth Regul. **21:** 383–415.

Bibikova, T.N., Zhigilei, A., and Gilroy, S. (1997). Root hair growth in *Arabidopsis thaliana* is directed by calcium and an endogenous polarity. Planta **203:** 495–505.

Bloch, D., Lavy, M., Efrat, Y., Efroni, I., Bracha-Drori, K., Abu-Abied, M., Sadot, E., and Yalovsky, S. (2005). Ectopic expression of an activated RAC in *Arabidopsis* disrupts membrane cycling. Mol. Biol. Cell **16:** 1913–1927.

Bloch, D., Monshausen, G., Singer, M., Gilroy, S., and Yalovsky, S. (2011). Nitrogen source interacts with ROP signalling in root hair tip-growth. Plant Cell Environ. **34:** 76–88.

Boeckstaens, M., André, B., and Marini, A.M. (2007). The yeast ammonium transport protein Mep2 and its positive regulator, the Npr1 kinase, play an important role in normal and pseudohyphal growth on various nitrogen media through retrieval of excreted ammonium. Mol. Microbiol. **64:** 534–546.

Boisson-Dernier, A., Roy, S., Kritsas, K., Grobei, M.A., Jaciubek, M., Schroeder, J.I., and Grossniklaus, U. (2009). Disruption of the pollen-expressed *FERONIA* homologs *ANXUR1* and *ANXUR2* triggers pollen tube discharge. Development **136:** 3279–3288.

Boron, W.F., and De Weer, P. (1976). Intracellular pH transients in squid giant axons caused by CO_2, NH_3, and metabolic inhibitors. J. Gen. Physiol. **67:** 91–112.

Britto, D.T., and Kronzucker, H.J. (2005). Nitrogen acquisition, PEP carboxylase, and cellular pH homeostasis: new views on old paradigms. Plant Cell Environ. **28:** 1396–1409.

Cárdenas, L., Feijo, J.A., Kunkel, J.G., Sanchez, F., Holdaway-Clarke, T., Hepler, P.K., and Quinto, C. (1999). Rhizobium nod factors induce increases in intracellular free calcium and extracellular calcium influxes in bean root hairs. Plant J. **19:** 347–352.

Carol, R.J., and Dolan, L. (2002). Building a hair: tip growth in *Arabidopsis thaliana* root hairs. Philos. Trans. R. Soc. Lond. B Biol. Sci. **357:** 815–821.

DeFalco, T.A., Bender, K.W., and Snedden, W.A. (2010). Breaking the code: Ca^{2+} sensors in plant signalling. Biochem. J. **425:** 27–40.

Dolan, L., Duckett, C.M., Grierson, C., Linstead, P., Schneider, K., Lawson, E., Dean, C., Poethig, S., and Roberts, K. (1994). Clonal origin and patterning in the root epidermis of *Arabidopsis.* Development **120:** 2465–2474.

Dolan, L., Janmaat, K., Willemsen, V., Linstead, P., Poethig, S., Roberts, K., and Scheres, B. (1993). Cellular organisation of the *Arabidopsis thaliana* root. Development **119:** 71–84.

Engelsberger, W.R., and Schulze, W.X. (2012). Nitrate and ammonium lead to distinct global dynamic phosphorylation patterns when resupplied to nitrogen-starved *Arabidopsis* seedlings. Plant J. **69:** 978–995.

Feller, A., Boeckstaens, M., Marini, A.M., and Dubois, E. (2006). Transduction of the nitrogen signal activating Gln3-mediated transcription is independent of Npr1 kinase and Rsp5-Bul1/2 ubiquitin ligase in *Saccharomyces cerevisiae.* J. Biol. Chem. **281:** 28546–28554.

Fentem, P.A., Lea, P.J., and Stewart, G.R. (1983). Ammonia assimilation in the roots of nitrate-and ammonia-grown *Hordeum vulgare* (cv Golden Promise). Plant Physiol. **71:** 496–501.

Finnemann, J., and Schjoerring, J.K. (1999). Translocation of NH_4^+ in oilseed rape plants in relation to glutamine synthetase isogene expression and activity. Physiol. Plant. **105:** 469–477.

Forde, B., and Lorenzo, H. (2001). The nutritional control of root development. Plant Soil **232:** 51–68.

Foreman, J., Demidchik, V., Bothwell, J.H., Mylona, P., Miedema, H., Torres, M.A., Linstead, P., Costa, S., Brownlee, C., Jones, J.D.G., Davies, J.M., and Dolan, L. (2003). Reactive oxygen species produced by NADPH oxidase regulate plant cell growth. Nature **422:** 442–446.

Gazzarrini, S., Lejay, L., Gojon, A., Ninnemann, O., Frommer, W.B., and von Wirén, N. (1999). Three functional transporters for constitutive, diurnally regulated, and starvation-induced uptake of ammonium into *Arabidopsis* roots. Plant Cell **11:** 937–948.

Gelli, A., and Blumwald, E. (1997). Hyperpolarization-activated Ca^{2+}-permeable channels in the plasma membrane of tomato cells. J. Membr. Biol. **155:** 35–45.

Gerendás, J., Zhu, Z., Bendixen, R., Ratcliffe, R.G., and Sattelmacher, B. (1997). Physiological and biochemical processes related to ammonium toxicity in higher plants. J. Plant Nutr. Soil Sci. **160:** 239–251.

Grierson, C., and Schiefelbein, J. (2009). Genetics of root hair formation. In Root Hairs, A.M.C. Emons and T. Ketelaar, eds (Berlin: Springer), pp. 1–25.

Grinstein, S., Romanek, R., and Rotstein, O.D. (1994). Method for manipulation of cytosolic pH in cells clamped in the whole cell or perforated-patch configurations. Am. J. Physiol. **267:** C1152–C1159.

Guo, H., Li, L., Ye, H., Yu, X., Algreen, A., and Yin, Y. (2009). Three related receptor-like kinases are required for optimal cell elongation in *Arabidopsis thaliana.* Proc. Natl. Acad. Sci. USA **106:** 7648–7653.

Hetherington, A.M., and Brownlee, C. (2004). The generation of Ca^{2+} signals in plants. Annu. Rev. Plant Biol. **55:** 401–427.

Hunter, P.R., Craddock, C.P., Di Benedetto, S., Roberts, L.M., and Frigerio, L. (2007). Fluorescent reporter proteins for the tonoplast and the vacuolar lumen identify a single vacuolar compartment in *Arabidopsis* cells. Plant Physiol. **145:** 1371–1382.

Ivashikina, N., Becker, D., Ache, P., Meyerhoff, O., Felle, H.H., and Hedrich, R. (2001). K^+ channel profile and electrical properties of *Arabidopsis* root hairs. FEBS Lett. **508:** 463–469.

Jones, M.A., Raymond, M.J., Yang, Z., and Smirnoff, N. (2007). NADPH oxidase-dependent reactive oxygen species formation required for root hair growth depends on ROP GTPase. J. Exp. Bot. **58:** 1261–1270.

Jones, M.A., Shen, J.J., Fu, Y., Li, H., Yang, Z., and Grierson, C.S. (2002). The *Arabidopsis* Rop2 GTPase is a positive regulator of both root hair initiation and tip growth. Plant Cell **14:** 763–776.

Kang, Y.H., Kirik, V., Hulskamp, M., Nam, K.H., Hagely, K., Lee, M.M., and Schiefelbein, J. (2009). The *MYB23* gene provides a positive feedback loop for cell fate specification in the *Arabidopsis* root epidermis. Plant Cell **21:** 1080–1094.

Kilian, J., Whitehead, D., Horak, J., Wanke, D., Weinl, S., Batistic, O., D'Angelo, C., Bornberg-Bauer, E., Kudla, J., and Harter, K. (2007). The AtGenExpress global stress expression data set: protocols, evaluation and model data analysis of UV-B light, drought and cold stress responses. Plant J. **50:** 347–363.

Klusener, B., and Weiler, E.W. (1999). A calcium-selective channel from root-Tip endomembranes of garden cress. Plant Physiol. **119:** 1399–1406.

Knight, H., Trewavas, A.J., and Knight, M.R. (1996). Cold calcium signaling in *Arabidopsis* involves two cellular pools and a change in calcium signature after acclimation. Plant Cell **8:** 489–503.

Knight, M.R., Campbell, A.K., Smith, S.M., and Trewavas, A.J. (1991). Transgenic plant aequorin reports the effects of touch and cold-shock and elicitors on cytoplasmic calcium. Nature **352:** 524–526.

Kwak, S.H., Shen, R., and Schiefelbein, J. (2005). Positional signaling mediated by a receptor-like kinase in *Arabidopsis.* Science **307:** 1111–1113.

Lanquar, V., Loqué, D., Hörmann, F., Yuan, L., Bohner, A., Engelsberger, W.R., Lalonde, S., Schulze, W.X., von Wirén, N., and Frommer, W.B. (2009). Feedback inhibition of ammonium uptake by a phospho-dependent allosteric mechanism in *Arabidopsis.* Plant Cell **21:** 3610–3622.

Laohavisit, A., et al. (2012). Arabidopsis annexin1 mediates the radical-activated plasma membrane Ca^{2+}- and K^+-permeable conductance in root cells. Plant Cell **24:** 1522–1533.

Lauter, F.R., Ninnemann, O., Bucher, M., Riesmeier, J.W., and Frommer, W.B. (1996). Preferential expression of an ammonium transporter and of two putative nitrate transporters in root hairs of tomato. Proc. Natl. Acad. Sci. USA **93:** 8139–8144.

Lee, M.M., and Schiefelbein, J. (1999). WEREWOLF, a MYB-related protein in *Arabidopsis*, is a position-dependent regulator of epidermal cell patterning. Cell **99:** 473–483.

Lee, R.B., and Ratcliffe, R.G. (1991). Observations on the subcellular distribution of the ammonium ion in maize root tissue using in-vivo ^{14}N-nuclear magnetic resonance spectroscopy. Planta **183:** 359–367.

Li, J.Y., et al. (2010). The *Arabidopsis* nitrate transporter NRT1.8 functions in nitrate removal from the xylem sap and mediates cadmium tolerance. Plant Cell **22:** 1633–1646.

Libault, M., Brechenmacher, L., Cheng, J., Xu, D., and Stacey, G. (2010). Root hair systems biology. Trends Plant Sci. **15:** 641–650.

López-Bucio, J., Cruz-Ramírez, A., and Herrera-Estrella, L. (2003). The role of nutrient availability in regulating root architecture. Curr. Opin. Plant Biol. **6:** 280–287.

Loqué, D., and von Wirén, N. (2004). Regulatory levels for the transport of ammonium in plant roots. J. Exp. Bot. **55:** 1293–1305.

Loqué, D., Ludewig, U., Yuan, L., and von Wirén, N. (2005). Tonoplast intrinsic proteins AtTIP2;1 and AtTIP2;3 facilitate NH_3 transport into the vacuole. Plant Physiol. **137:** 671–680.

Loqué, D., Mora, S.I., Andrade, S.L., Pantoja, O., and Frommer, W.B. (2009). Pore mutations in ammonium transporter AMT1 with increased electrogenic ammonium transport activity. J. Biol. Chem. **284:** 24988–24995.

Loqué, D., Yuan, L., Kojima, S., Gojon, A., Wirth, J., Gazzarrini, S., Ishiyama, K., Takahashi, H., and von Wirén, N. (2006). Additive contribution of AMT1;1 and AMT1;3 to high-affinity ammonium uptake across the plasma membrane of nitrogen-deficient *Arabidopsis* roots. Plant J. **48:** 522–534.

Lorenz, M.C., and Heitman, J. (1998). The MEP2 ammonium permease regulates pseudohyphal differentiation in *Saccharomyces cerevisiae.* EMBO J. **17:** 1236–1247.

Ludewig, U., von Wirén, N., and Frommer, W.B. (2002). Uniport of NH_4^+ by the root hair plasma membrane ammonium transporter LeAMT1;1. J. Biol. Chem. **277:** 13548–13555.

Ludewig, U., Wilken, S., Wu, B., Jost, W., Obrdlik, P., El Bakkoury, M., Marini, A.M., André, B., Hamacher, T., Boles, E., von Wirén, N., and Frommer, W.B. (2003). Homo- and hetero-oligomerization of ammonium transporter-1 NH_4^+ uniporters. J. Biol. Chem. **278:** 45603–45610.

Marini, A.M., Vissers, S., Urrestarazu, A., and André, B. (1994). Cloning and expression of the *MEP1* gene encoding an ammonium transporter in *Saccharomyces cerevisiae.* EMBO J. **13:** 3456–3463.

McAinsh, M.R., Brownlee, C., and Hetherington, A.M. (1992). Visualizing changes in cytosolic-free Ca^{2+} during the response of stomatal guard cells to abscisic acid. Plant Cell **4:** 1113–1122.

Monshausen, G.B., Bibikova, T.N., Messerli, M.A., Shi, C., and Gilroy, S. (2007). Oscillations in extracellular pH and reactive oxygen species modulate tip growth of *Arabidopsis* root hairs. Proc. Natl. Acad. Sci. USA **104:** 20996–21001.

Monshausen, G.B., Messerli, M.A., and Gilroy, S. (2008). Imaging of the Yellow Cameleon 3.6 indicator reveals that elevations in cytosolic Ca^{2+} follow oscillating increases in growth in root hairs of *Arabidopsis.* Plant Physiol. **147:** 1690–1698.

Moseyko, N., and Feldman, L.J. (2001). Expression of pH-sensitive green fluorescent protein in *Arabidopsis thaliana.* Plant Cell Environ. **24:** 557–563.

Murata, Y., Pei, Z.M., Mori, I.C., and Schroeder, J. (2001). Abscisic acid activation of plasma membrane Ca^{2+} channels in guard cells requires cytosolic NAD(P)H and is differentially disrupted upstream and downstream of reactive oxygen species production in *abi1-1* and *abi2-1* protein phosphatase 2C mutants. Plant Cell **13:** 2513–2523.

Pearson, J., and Stewart, G.R. (1993). The deposition of atmospheric ammonia and its effects on plants. New Phytol. **125:** 283–305.

Peck, S.C. (2006). Analysis of protein phosphorylation: methods and strategies for studying kinases and substrates. Plant J. **45:** 512–522.

Peiter, E., Maathuis, F.J.M., Mills, L.N., Knight, H., Pelloux, J., Hetherington, A.M., and Sanders, D. (2005). The vacuolar Ca^{2+}-activated channel TPC1 regulates germination and stomatal movement. Nature **434:** 404–408.

Pitts, R.J., Cernac, A., and Estelle, M. (1998). Auxin and ethylene promote root hair elongation in *Arabidopsis.* Plant J. **16:** 553–560.

Rentel, M.C., Lecourieux, D., Ouaked, F., Usher, S.L., Petersen, L., Okamoto, H., Knight, H., Peck, S.C., Grierson, C.S., Hirt, H., and Knight, M.R. (2004). OXI1 kinase is necessary for oxidative burst-mediated signalling in *Arabidopsis.* Nature **427:** 858–861.

Schiefelbein, J.W., Shipley, A., and Rowse, P. (1992). Calcium influx at the tip of growing root-hair cells of *Arabidopsis thaliana.* Planta **187:** 455–459.

Schneider, K., Mathur, J., Boudonck, K., Wells, B., Dolan, L., and Roberts, K. (1998). The *ROOT HAIRLESS 1* gene encodes a nuclear protein required for root hair initiation in *Arabidopsis.* Genes Dev. **12:** 2013–2021.

Song, C.P., Agarwal, M., Ohta, M., Guo, Y., Halfter, U., Wang, P., and Zhu, J.K. (2005). Role of an *Arabidopsis* AP2/EREBP-type transcriptional repressor in abscisic acid and drought stress responses. Plant Cell **17:** 2384–2396.

Speer, M., Brune, A., and Kaiser, W.M. (1994). Replacement of nitrate by ammonium as the nitrogen source increases the salt sensitivity of pea plants. 1. Ion concentrations in roots and leaves. Plant Cell Environ. **17:** 1215–1221.

Van Zeebroeck, G., Kimpe, M., Vandormael, P., and Thevelein, J.M. (2011). A split-ubiquitin two-hybrid screen for proteins physically interacting with the yeast amino acid transceptor Gap1 and ammonium transceptor Mep2. PLoS ONE **6:** e24275.

Véry, A.A., and Davies, J.M. (2000). Hyperpolarization-activated calcium channels at the tip of *Arabidopsis* root hairs. Proc. Natl. Acad. Sci. USA **97:** 9801–9806.

Wang, M.Y., Siddiqi, M.Y., Ruth, T.J., and Glass, A.D. (1993). Ammonium uptake by rice roots (I. Fluxes and subcellular distribution of $^{13}NH_4^+$). Plant Physiol. **103:** 1249–1258.

Warth, R., et al. (2004). Proximal renal tubular acidosis in TASK2 K^+ channel-deficient mice reveals a mechanism for stabilizing bicarbonate transport. Proc. Natl. Acad. Sci. USA **101:** 8215–8220.

Wells, D.M., and Miller, A.J. (2000). Intracellular measurement of ammonium in *Chara corallina* using ion-selective microelectrodes. Plant Soil **221:** 103–106.

Wymer, C.L., Bibikova, T.N., and Gilroy, S. (1997). Cytoplasmic free calcium distributions during the development of root hairs of *Arabidopsis thaliana.* Plant J. **12:** 427–439.

Yoo, S.D., Cho, Y.H., and Sheen, J. (2007). *Arabidopsis* mesophyll protoplasts: a versatile cell system for transient gene expression analysis. Nat. Protoc. **2:** 1565–1572.

Yuan, L., Loqué, D., Kojima, S., Rauch, S., Ishiyama, K., Inoue, E., Takahashi, H., and von Wirén, N. (2007). The organization of high-affinity ammonium uptake in *Arabidopsis* roots depends on the spatial arrangement and biochemical properties of AMT1-type transporters. Plant Cell **19:** 2636–2652.

Zhang, X., Miao, Y.C., An, G.Y., Zhou, Y., Shangguan, Z.P., Gao, J.F., and Song, C.P. (2001). K^+ channels inhibited by hydrogen peroxide mediate abscisic acid signaling in *Vicia* guard cells. Cell Res. **11:** 195–202.